Journal of Electroceramics, 14, 265–271, 2005

Site Preference of La in $Bi_{3.75}La_{0.25}Ti_3O_{12}$ Using Neutron Powder Diffraction and Raman Scattering

YONG-IL KIM,[1,*,†] SEUNG-HOON NAHM,[1] DONG-JIN YOON[1] & DUNCAN H. GREGORY[2]

[1] *Korea Research Institute of Standards and Science, P.O. Box 102, Yuseong, Daejeon, 305-600, Republic of Korea*
[2] *School of Chemistry, University of Nottingham, Nottingham, NG7 2RD, UK*

Submitted June 21, 2004; Revised December 23, 2004; Accepted December 30, 2004

Abstract. Both structural refinement using neutron powder diffraction data and Raman scattering were carried out to determine the site preference of La atoms and the cation distribution in $Bi_{3.75}La_{0.25}Ti_3O_{12}$ compound. Of three possible cation-disorder models, the best structural refinement result was obtained from a model that La atoms substitute only for Bi atoms outside of the TiO_6 octahedra in the $Bi_2Ti_3O_{10}$ unit. The model proposed by the structural refinement was corroborated by the Raman spectroscopic study. The final weighted R-factor, R_{wp}, and the goodness-of-fit indicator, $S\ (=R_{wp}/R_e)$, based on the neutron diffraction and the Raman scattering were 4.12% and 1.43, respectively. The occupancy of La atoms for two Bi sites in the perovskite-like unit was 0.082 and 0.074, respectively. The refined model described a structure in monoclinic space group $B1a1$ with $Z = 4$, $a = 5.4387(1)$ Å, $b = 5.4129(1)$ Å, $c = 32.8441(1)$ Å and $\beta = 90.03(1)°$.

Keywords: ferroelectric material, $Bi_{3.75}La_{0.25}Ti_3O_{12}$, structural refinement, neutron powder scattering, Raman sctteering

1. Introduction

Layered perovskite materials such as $SrBi_2Ta_2O_9$, $Bi_4Ti_3O_{12}$, $Bi_{3.25}La_{0.75}Ti_3O_{12}$ and $Bi_{3.15}Nd_{0.85}Ti_3O_{12}$ show good fatigue characteristics compared to $Pb(Zr_xTi_{1-x})O_3$ using metal electrodes [1, 2]. One of these layered materials, $Bi_{3.75}La_{0.25}Ti_3O_{12}$ (BLT), has attracted strong interest because it can be crystallized at a temperatures compatible with silicon based integrated circuit techniques and shows fatigue free properties [3–5].

Although many reports have noted that La atoms possibly play a key role in the fatigue free characteristics of $Bi_{4-x}La_xTi_3O_{12}$, most of the studies concerning the amount of La atoms substituting for Bi atoms have focused chemically on the quantities of La atoms in the compound. Determining the quantities of La atoms in the crystal lattice is an important thing because the amount of La atoms doped into the crystal lattice of $Bi_4Ti_3O_{12}$(BTO) is directly related to the remnant polarization and the fatigue properties of BLT. Furthermore, the crystal structural information of BLT is important to understand the behavior of spontaneous polarization at room temperature and to guide the growth direction of BLT thin films. However, structural study of BLT and reported results are lacking relative to research on preparation methods and the characterization of electrical and physical properties for the BLT compound.

The present study is focused on the determination of the site preference of La atoms in BLT compound by means of the structural refinement using neutron powder diffraction data and Raman spectroscopy. The neutron powder diffraction experiment is useful to obtain the information of oxygen atoms in oxide compounds. The Raman spectroscopy is sensitive to the coordination of local sites caused by the distortion of polyhedron or the atomic substitution because its spectrum is originated from the lattice vibrational

---

*To whom all correspondence should be addressed. E-mail: yikim@kriss.re.kr

†*Present address*: School of Chemistry, University of Nottingham, Nottingham, NG7 2RD, UK.

modes depending on the atomic masses of constituent atoms.

2. Experimental

The BTO and BLT samples were prepared by a normal solid-state reaction using Bi_2O_3(99.99%, Aldrich), TiO_2(99.9%, Aldrich) and La_2O_3 (99.99%, Aldrich) as starting materials. Stoichiometric quantities of Bi_2O_3, TiO_2 and La_2O_3 were mixed and ground. The mixture was annealed at 1050°C for 17 h. A second annealing process was performed for 48 h at 1200°C.

The neutron powder diffraction data were collected over scattering angles ranging from 0°–160° using 1.8348 Å neutron on the samples a High Resolution Powder Diffractometer (HRPD) at Hanaro Center of the Korea Atomic Energy Research Institute. The General Structure Analysis System (GSAS) program was used to do the structural refinement [6]. The pseudo-Voigt function among profile functions in GSAS program was chosen for the simualtion of the peak shape with two component defining Gaussian and Lorentzian character of the peaks as a function of 2θ [7]. Raman spectroscopy with 1064 nm lines of exciting source from an Nd-YAG laser were used to both the phase identification and the site preference of La atoms.

3. Results and Discussion

BTO has two kinds of crystal systems, monoclinic and orthorhombic, at room temperature [8, 9]. According to the Rietveld refinement of BTO using neutron powder diffraction data [10–12], the monoclinic system with space group $B1a1$ was more suitable than the orthorhombic system as a crystal system at room temperature. All the peaks of the BLT sample could be indexed based on the monoclinic crystal system. Therefore, the monoclinic system with the space group of $B1a1$ (no. 7, non-standard setting of $P1c1$) like BTO was used as an initial structural model for BLT in this study.

Three types of substitutions of La atoms for Bi atoms in BLT are possible. La atoms may substitute for Bi atoms in either only the Bi_2O_2 layer (L-model) or only the perovskite-like unit, $Bi_2Ti_3O_{10}$ (P-model). It is also possible that Bi atoms are partially substituted into both the Bi_2O_2 layer and the perovskite-like unit (B-model). On the assumption that the occupancies of Bi and La sites in all models were constrained so that both sites were fully occupied, and the total occupancy of Bi and La atoms was maintained to be unity, the initial structural refinement for all models was done by the unit-cell, the zero-point shift, and background parameters. After a match of peak positions was achieved, peak profile parameters including the peak asymmetry were refined. α-Al_2O_3 powder was used as an external standard to correct the zero-point shift for the measured diffraction data.

Figure 1 shows the structural refinement patterns of BLT for the aforementioned three models. The converged weighted R-factors, R_{wp}, which are calculated from the differences between the observed and calculated data, for L-, P- and B-models were 4.20, 4.12 and 4.18%, respectively. Also, the goodness-of-fit indicator, S $(=R_{wp}/R_e)$, for L-, P- and B-models was 1.47, 1.43 and 1.46, respectively. In general, the structural refinement adopts numerical criteria, e.g. R_{wp}, R_p, R_B, R_F, R_e and S, to make a judgment in the structural refinement whether a crystal structural model is adequate or not, Among them, the most meaningful indices are R_{wp} and S because they show in the numerator for quantity being minimized [13]. Considering the final converged R-factors and goodness-of-fit indicator for the three models, the differences between the models are subtle. Nevertheless, it can be concluded that the P-model appears to be the most suitable representation of La atom in BLT at room temperature. The number of refined parameters for individual model including profile function parameters was 99.

Raman spectroscopy was chosen as a complementary method to provide further evidence for the site preference of La atoms in BLT because it is sensitive to the change of local structure resulting from atomic substitutions and distortion of polyhedra. Figure 2 shows the Raman scattering spectra of BTO (closed circles) and BLT (open circles) at room temperature. The vibrational modes of BTO can be classified into the lattice transitions involved in the displacement of cations and the internal modes of TiO_6 octahedra [14–17]. Taking into account the effect of atomic mass on the vibrational modes in BLT, the low-frequency modes may be attributed to the motion of Bi atoms. Conversely internal vibrational modes of TiO_6 octahedra are expected to appear above 200 cm^{-1}. The six expected peaks appeared at 228, 269, 333, 535, 616 and 850 cm^{-1} are caused by the internal vibrational modes of TiO_6 octahedra. Bands below 200 cm^{-1} are ascribed to two different Bi sites, those within the Bi_2O_2 layer and those in the perovskite-like unit. The band

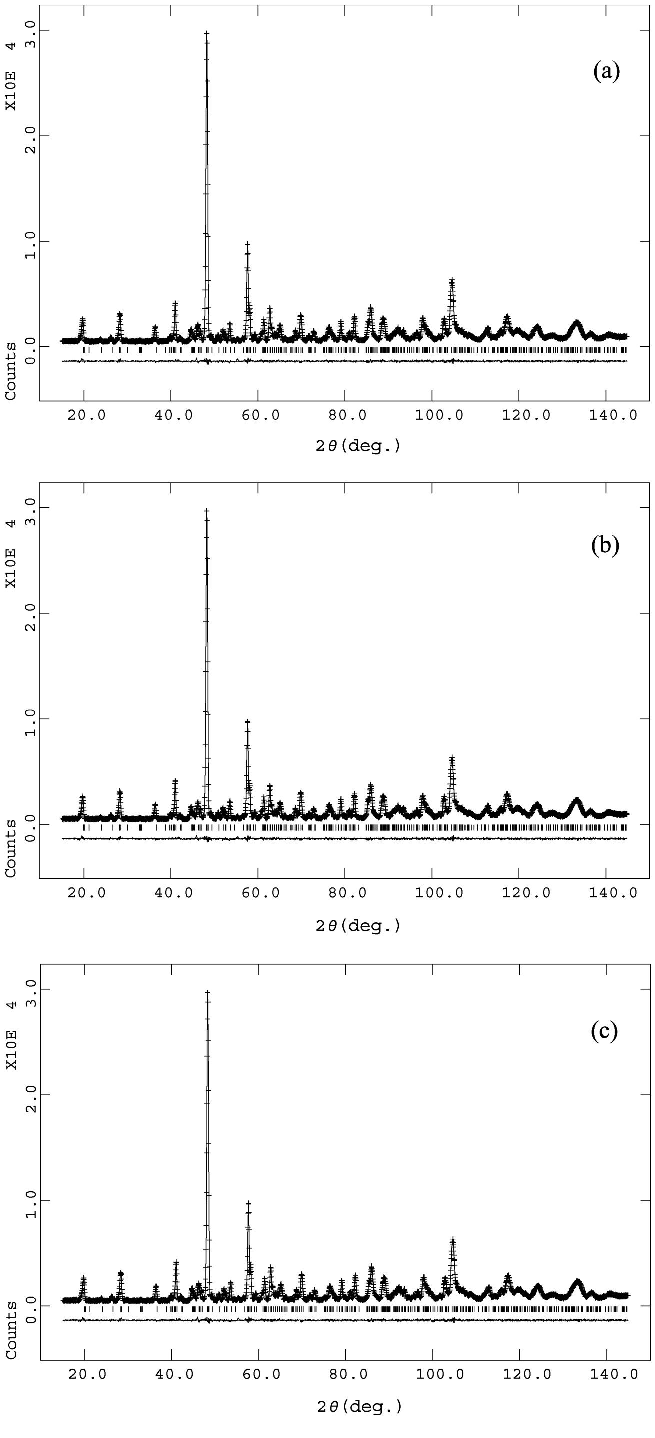

Fig. 1. The structural refinement patterns of $Bi_{3.75}La_{0.25}Ti_3O_{12}$ for three models at room temperature: (a) the L-model (La atoms substitute for Bi atoms in the Bi_2O_2 layer), (b) the P-model (La atoms substitute for Bi atoms in the perovskite-like unit, $Bi_2Ti_3O_{10}$) and (c) the B-model (La atoms partially substitute for Bi atoms of both Bi_2O_2 layer and of $Bi_2Ti_3O_{10}$ unit). Plus (+) marks represent the observed intensities, and the solid line defines calculated ones. A difference (obs. – cal.) plot is shown beneath. Tick marks above the difference indicate the reflection positions.

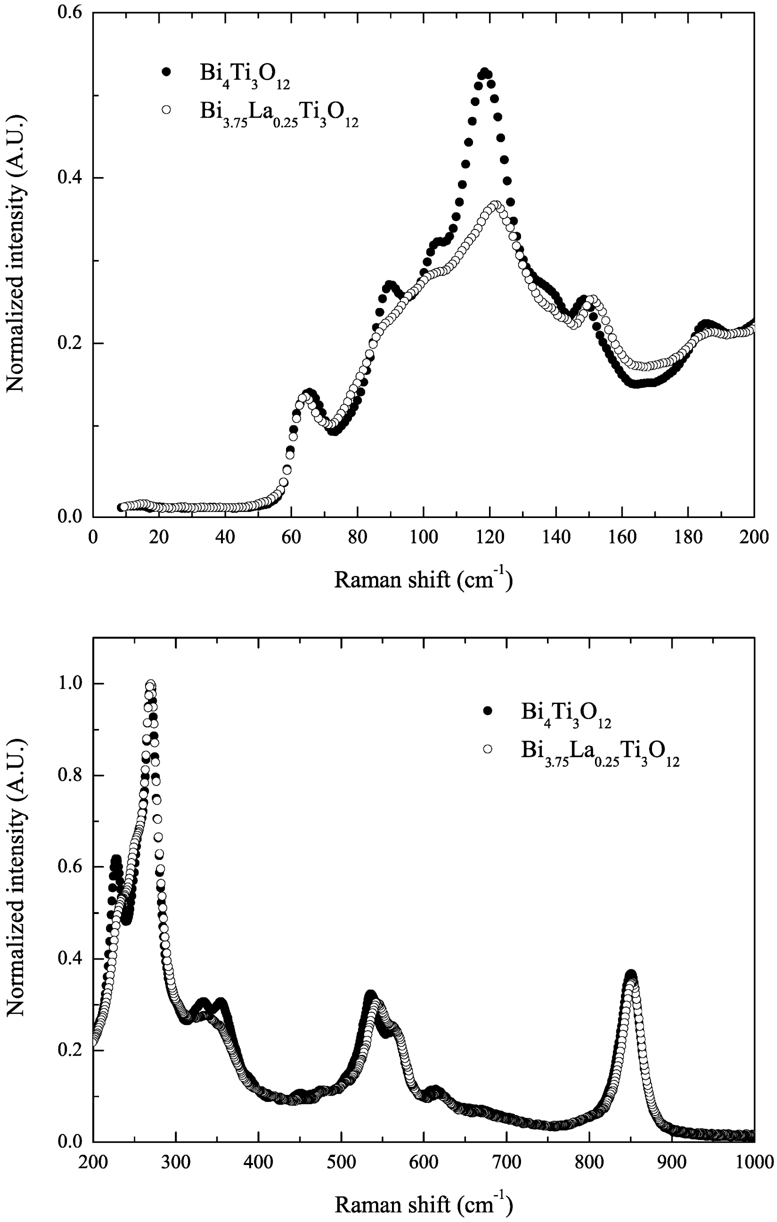

Fig. 2. The Raman scattering spectra of $Bi_4Ti_3O_{12}$ (colsed circles) and $Bi_{3.75}La_{0.25}Ti_3O_{12}$ (open circles) at room temperature.

at 65 cm^{-1} (L-mode) is assigned as a rigid-layer mode which originates from Bi displacement in the Bi_2O_2 layer. The three peaks (P-mode) at 90, 119 and 148 cm^{-1} are related to the Bi atoms in the perovskite-like unit.

As shown in Fig. 2, in comparison with the Raman spectrum of BTO, while the change in L-mode of BLT was very small, the peaks of P-mode were remarkably shifted to higher frequencies. The first peak of P-mode corresponding to 90 cm^{-1} of BTO was too diffusive to determine the precise peak position. However, the peaks at 119 and 148 cm^{-1} for BTO are clearly moved to the higher frequencies of 122 and 151 cm^{-1} in BLT. The Raman peak shifts toward higher frequency signify that atoms of lighter atomic weight have substituted into the modified material.

Table 1. Refined structural parameters for $Bi_{3.75}La_{0.25}Ti_3O_{12}$ obtained from the structural refinement using neutron powder diffraction data at room temperature. The symbol, g and U_{iso}, represent the occupation factor and the isotropic thermal parameter. The numbers in parentheses are the estimated standard deviations of the last significant figure.

Atom	Site	x	y	z	g	$100*U_{iso}/Å^2$
Bi(a)	4*a*	0.0415 (16)	0.5044 (9)	0.5647 (2)	0.918 (3)	1.61 (16)
La(a)	4*a*	0.0415 (16)	0.5044 (9)	0.5647 (2)	0.082	1.61 (16)
Bi(a)	4*a*	0.0413 (12)	0.4898 (8)	0.7106 (1)	1.0	0.91 (14)
Ti(a)	4*a*	0.0832 (16)	−0.0183 (7)	0.5026 (2)	1.0	0.13 (12)
Ti(a)	4*a*	0.0779 (14)	−0.0124 (15)	0.6246 (1)	1.0	0.01 (16)
O(a)	4*a*	0.3266 (11)	0.2773 (18)	0.5063 (2)	1.0	2.96 (20)
O(a)	4*a*	0.3199 (15)	0.2469 (15)	0.2500 (2)	1.0	0.31 (11)
O(a)	4*a*	0.1225 (15)	−0.0674 (14)	0.5578 (1)	1.0	0.56 (17)
O(a)	4*a*	0.0952 (12)	0.0646 (15)	0.6798 (2)	1.0	0.60 (19)
O(a)	4*a*	0.3323 (17)	0.2644 (11)	0.6095 (1)	1.0	1.67 (16)
O(a)	4*a*	0.4015 (14)	−0.2001 (12)	0.6227 (2)	1.0	1.79 (20)
Bi(b)	4*a*	0.0467 (16)	0.4920 (10)	0.4312 (2)	0.926 (2)	0.81 (15)
La(b)	4*a*	0.0467 (16)	0.4920 (10)	0.4312 (2)	0.074	0.81 (15)
Bi(b)	4*a*	0.0395 (16)	0.5297 (11)	0.2877 (1)	1.0	1.43 (10)
Ti(b)	4*a*	0.0919 (14)	−0.0079 (18)	0.3679 (2)	1.0	0.54 (20)
O(b)	4*a*	0.3881 (11)	−0.2198 (14)	0.4919 (1)	1.0	1.57 (19)
O(b)	4*a*	0.3082 (12)	−0.2456 (11)	0.7496 (2)	1.0	0.64 (12)
O(b)	4*a*	0.1190 (11)	0.0529 (11)	0.4403 (1)	1.0	0.02 (16)
O(b)	4*a*	0.0727 (12)	−0.0189 (12)	0.3172 (1)	1.0	2.70 (16)
O(b)	4*a*	0.3222 (12)	−0.2771 (14)	0.3847 (2)	1.0	1.22 (15)
O(b)	4*a*	0.3617 (11)	0.2171 (14)	0.3759 (1)	1.0	2.28 (20)

(a) Constraint on atomic coordinate: $x(\mathrm{Bi}) = x(\mathrm{La})$, $y(\mathrm{Bi}) = y(\mathrm{La})$ and $z(\mathrm{Bi}) = z(\mathrm{La})$.
(b) Constraint on occupancy: $g(\mathrm{Bi}) + g(\mathrm{La}) = 1.0$.
(c) Constraint on isotropic temperature factor: $U_{iso}(\mathrm{Bi}) = U_{iso}(\mathrm{La})$.

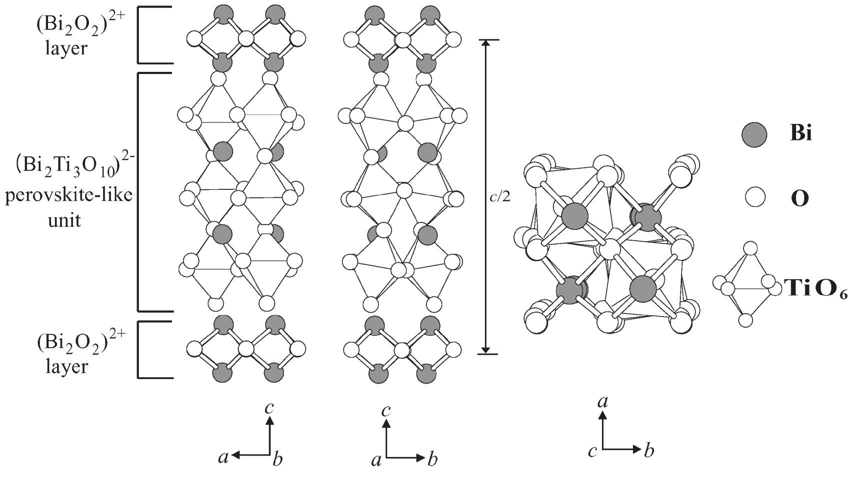

Fig. 3. The crystal structure of $Bi_{3.75}La_{0.25}Ti_3O_{12}$ based on the refined structural parameters obtained from the structural refinement at room temperature.

Therefore, the increase in wavenumbers for the P-mode in BLT suggests that the preferred substitution site of La atoms is at the Bi atomic sites of the perovskite-like unit, $Bi_2Ti_3O_{10}$. The Raman results thus support the crystal structure model (P-model), where the doped La atoms were substituted for the Bi atoms of the perovskite-like unit. The changes above 200 cm^{-1} in BLT are caused by the relaxation of the

Table 2. Selected interatomic distances and bond angles for $Bi_{3.75}La_{0.25}Ti_3O_{12}$ (P-model)at room temperatutre

Bond	Distance(Å)	Bond	Distance(Å)	Bond	Distance(Å)
M(1)$^{i)}$-O1(a)	2.763 (1)	M(1)-O1(a)	2.714 (2)	M(1)-O3(a)	3.111 (1)
M(1)-O3(a)	2.395 (1)	M(1)-O3(a)	2.312 (1)	M(1)-O3(a)	3.118 (2)
M(1)-O5(a)	2.485 (1)	M(1)-O5(a)	2.385 (2)	M(1)-O6(a)	3.184 (1)
M(1)-O6(a)	2.289 (2)	M(1)-O7(b)	3.387 (1)	M(1)-O7(b)	2.804 (2)
M(2)$^{ii)}$-O1(a)	3.130(2)	M(2)-O1(a)	3.100(1)	M(2)-O7(b)	3.124 (1)
M(2)-O7(b)	2.498 (1)	M(2)-O9(b)	2.412 (1)	M(2)-O9(b)	3.094 (1)
M(2)-O9(b)	2.355 (1)	M(2)-O9(b)	3.147 (2)	M(2)-O11(b)	2.486 (2)
M(2)-O11(b)	2.445 (1)	M(2)-O12(b)	2.946 (1)	M(2)-O12(b)	2.361 (2)
Bi2(a)-O2(a)	2.199 (2)	Bi2(a)-O2(a)	2.350 (1)	Bi2(a)-O4(a)	2.528 (2)
Bi2(a)-O4(a)	3.272 (1)	Bi2(a)-O4(a)	2.679 (2)	Bi2(a)-O4(a)	3.1431 (1)
Bi2(a)-O6(a)	3.192 (2)	Bi2(a)-O8(b)	2.375 (1)	Bi2(a)-O8(b)	2.296 (2)
Bi4(b)-O2(a)	2.515 (1)	Bi4(b)-O2(a)	2.281 (1)	Bi4(b)-O8(b)	2.146 (2)
Bi4(b)-O8(b)	2.282 (1)	Bi4(b)-O10(b)	3.129 (1)	Bi4(b)-O10(b)	2.637 (1)
Bi4(b)-O10(b)	2.649 (1)	Bi4(b)-O10(b)	3.121 (2)	Bi4(b)-O12(b)	3.316 (1)
Ti1(a)-O1(a)	1.939 (2)	Ti1(a)-O1(a)	1.757(1)	Ti1(a)-O3(a)	1.907 (1)
Ti1(a)-O7(b)	2.146 (1)	Ti1(a)-O7(b)	1.964 (2)	Ti1(a)-O10(b)	2.045 (1)
Ti2(a)-O3(a)	2.260 (1)	Ti2(a)-O4(a)	1.833 (1)	Ti2(a)-O5(a)	2.100 (2)
Ti2(a)-O5(a)	1.950 (1)	Ti2(a)-O6(a)	2.036 (2)	Ti2(a)-O6(a)	1.865 (1)
Ti3(b)-O9(b)	2.379 (2)	Ti3(b)-O10(b)	1.700 (1)	Ti3(b)-O11(b)	2.000 (1)
Ti3(b)-O11(b)	1.986 (1)	Ti3(b)-O12(b)	1.946 (2)	Ti3(b)-O12(b)	1.963 (1)

Bond type	angle (°)	Bond type	angle (°)
O1(a)-Ti1(a)-O1(b)	167.50 (1)	O1(a)-Til(a)-O1(b)	175.73 (1)
O3(a)-Ti1(a)-O4(b)	164.26 (1)	O3(a)-Ti2(a)-O4(a)	171.21 (1)
O5(a)-Ti2(a)-O6(a)	159.25 (1)	O5(a)-Ti2(a)-O6(a)	157.02 (1)
O3(b)-Ti1(b)-O4(b)	174.71 (1)	O5(b)-Ti1(b)-O6(b)	157.25 (1)
O5(b)-Ti1(b)-O6(b)	157.14 (1)		

(i) M(1) : Bi1(a) or La1(a).
(ii) M(2) : Bi3(b) or La2(b).

structural distortion and the decrease of TiO_6 octahedral tilting.

The refined structural parameters, the selected atomic distances and angles based on the P-model are given in Tables 1 and 2, respectively. The structural refinement results show that the La atoms are disordered over two fourfold symmetry Bi sites in the perovskite-like unit, $4f$ site, and that the occupancy of substituting La atoms for Bi atoms in the perovskite-like unit is 0.082(3) and 0.074(2), respectively. The refined lattice constants were $a = 5.4387(1)$ Å, $b = 5.4129(1)$Å, $c = 32.8441(1)$Å) and $\beta = 90.03(1)°$. The crystal structure of BLT based on the refined structural parameters is illustrated in Fig. 3. Compared with the ideal tetragonal structure of the Aurivillius phases, the Bi_2O_2 layers and TiO_6 octahedra are distorted. The TiO_6 octahedra along the c-axis are buckled.

4. Conclusion

A combined structural study by Raman spectroscopy and the structural refinement using neutron powder diffraction data was successfully performed to determine the site preference of La atoms in $Bi_{3.75}La_{0.25}Ti_3O_{12}$ synthesized by high temperature solid-state reaction. Of three possible cation-disorder models, the best refinement result was obtained from a model where the doped La atoms substitute only for the Bi atoms in the perovskite-like unit, $Bi_2Ti_3O_{10}$. The final weighted R-factor and the goodness-of-fit were 4.12% and 1.43, respectively. The model could be corroborated by Raman spectroscopy in that the three bands related to the Bi atoms in the perovskite-like unit were shifted to the higher frequencies, indicating the substitution of La at these Bi positions.

Acknowledgments

The authors are grateful to Dr. Y. N. Choi at the Hanaro Center of the Korea Atomic Energy Research Institute. Also, we acknowledge the Ministry of Science and Technology of Korea for financial support through Centre for Nanoscale Mechatronics and Manufacturing.

References

1. C.A-Paz de Araujo, J.D. Cuchiaro, L.D. McMillan, M.C. Scott, and J.F. Scott, *Nature*, **374**, 627 (1995).
2. R. Ramesh, S. Aggarwal, and O. Auciello, *Mat. Sci. Eng.*, **32**, 191 (2001).
3. T. Kijima, M. Ushikubo, and H. Matsunaga, *Jpn. J. Appl. Phys.*, **38**, 127 (1999).
4. B.H. Park, B.S. Kang, S.D. Bu, T.W. Noh, J. Lee, and W. Jo, *Nature*, **401**, 682 (1999).
5. U. Chon, G.C. Yi, and H.M. Jang, *Appl. Phys. Lett.*, **78**, 658 (2001).
6. A.C. Larson and R.B. Von Dreele, Los Alamos National Laboratory Report LAUR, 86–748 (1994).
7. L.W. Finger, D.E. Cox, and A.P. Jephcoat, *J Appl. Cryst.*, **27**, 892 (1994).
8. A.D. Rae, J.G. Thompson, R.L. Withers, and A.C. Willis, *Acta Cryst.*, **B46**, 474 (1990).
9. C.H. Hervoches and P. Lightfoot, *Chem. Mater.*, **11**, 3359 (1999).
10. Y. Shimakawa, Y. Kubo, Y. Tauchi, S. Asano, T. Kamiyama, F. Izumi, and Z. Hiroi, *Appl. Phys. Lett.*, **79**, 2791 (2001).
11. Y.I. Kim, M.K. Jeon, and S.I. Woo, *J. Mater. Sci. Lett.*, **22**, 1655 (2003).
12. Y.I. Kim and M.K. Jeon, *Mater. Lett.*, **58**, 1889 (2004).
13. R.A. Young, *The Rietveld Method* (Oxford University Press, Oxford, 1993), Chap. 1.
14. M. Osada, M. Tada, M. Kakihana, T. Watanabe, and H. Funakubo, *Jpn. J. Appl. Phys.*, **40**, 5572 (2001).
15. M.S. Tomar, R.E. Melgarejo, A. Hidalgo, S.B. Mazumder, and R.S. Katiyar, *J. Appl. Phys.*, **83**, 341 (2003).
16. S. Kojima, R. Imaizumi, S. Hamazaki, and M. Takashige, *Jpn. J. Appl. Phys.*, **33**, 5559 (1994).
17. S. Kojima and S. Shimada, *Physica B*, **219–220**, 617 (1996).